

Original

## Heat Stress in Rat Adriamycin Cardiomyopathy: Heat Shock Protein 25 and Myosin Accumulation

Mirian Strauss<sup>1</sup>, Alegna Rada<sup>1</sup>, Félix Tejero<sup>2</sup>, and Tomás Hermoso<sup>3</sup>

<sup>1</sup>Sección de Biología Celular, Instituto de Medicina Tropical, Facultad de Medicina Universidad Central de Venezuela, Caracas 1041A, Venezuela

<sup>2</sup>Instituto de Zoología y Ecología Tropical, Facultad de Ciencias. Universidad Central de Venezuela, Caracas 1041A, Venezuela

<sup>3</sup>Sección de Bioquímica de Parásitos, Instituto de Medicina Tropical, Facultad de Medicina, Universidad Central de Venezuela, Caracas 1041A, Venezuela

**Abstract:** In order to evaluate the effects of hyperthermia on adriamycin cardiomyopathy and its relationship with heat shock protein induction and myosin accumulation, female Sprague-Dawley rats (21–24 days) were randomized into four groups: the control, adriamycin, temperature and temperature-adriamycin groups. Adriamycin was injected i.v. at a dose of 27 mg/Kg (0.1 ml). The rats were exposed to a temperature of 45°C for 35 min, followed by a recovery (1 h) at room temperature prior to adriamycin treatment. Body weight was recorded weekly. The thickness of the ventricular wall and percentage of cellular damage were biometrically and ultrastructurally evaluated, respectively. Heat shock protein 25 and myosin accumulation were determined through Western blot analysis. The determinations were carried out monthly until the third month after treatment. At eight and twelve weeks after treatment, the thickness of the ventricular wall seemed to decrease in the adriamycin-treated rats in relation to the other groups. An electron microscopic analysis of the adriamycin group's left ventricular wall samples, showed more sarcomeric changes and loss of myofibrils than the control, temperature and temperature-adriamycin groups. At 24 hours after treatment with adriamycin, higher levels of heat shock protein 25 and myosin were observed (week 0) in the temperature-adriamycin group than in the control and adriamycin groups (4, 8 and 12 weeks). Hyperthermia was confirmed by a multivariate approach to induce heat shock protein 25 and myosin, which would strengthen cardiac-sarcomeric myosin arrangement. (*J Toxicol Pathol* 2010; 23: 235–243)

**Key words:** hyperthermia, heat shock protein 25, myosin, adriamycin cardiomyopathy, left ventricular wall thickness, cellular damage

### Introduction

The clinical efficacy of the antitumor antibiotic drug adriamycin is severely limited by its cardiotoxic effects<sup>1,2</sup>. In an experimental rat model of cardiomyopathy, this potent cardiotoxin causes a significant reduction in body weight, left ventricular wall thickness and heat shock protein 70 and 25 (Hsp70, Hsp25) accumulations<sup>3</sup>. Moreover, the ventricular action potential duration is significantly shortened in the presence of adriamycin, while the incidence of ventricular fibrillation is significantly enhanced<sup>4</sup>. All this, as well as serious degenerations at the subcellular level, have previously been demonstrated<sup>3</sup>.

In this regard, selective inhibition of cardiac muscle

gene expression is among the earliest events in adriamycin cardiotoxicity, which may lead to mostly irreversible and sometimes fatal cardiomyopathy in patients treated with adriamycin<sup>5,6</sup>. Furthermore, rats injected with adriamycin showed a dose-dependent decrease in the levels of mRNAs for alpha-actin, troponin I, myosin light chain 2 and M isoform of creatine kinase in cardiac muscles. These selective changes in gene expression in cardiocyte cultures and cardiac muscles precede classical ultrastructural changes and may explain the myofibrillar loss that characterizes adriamycin cardiac injury<sup>7</sup>. In this sense, different cardioprotective strategies have been evaluated, including L-carnitine, which reduces the severity of late adriamycin cardiomyopathy, by promoting the induction of Hsp25<sup>3</sup>.

Heat stress is associated with the induction of heat shock proteins (Hsps), which in turn modulates cellular survival or death<sup>8</sup>. In vitro results show that heat shock induced-Hsp27 can protect against adriamycin induced toxicity in cardiac H9c2 cells<sup>9</sup>. The depletion of Hsp27 in cardiac H9c2 cells by small interfering siRNA also reduced the

---

Received: 10 June 2010, Accepted: 6 September 2010

Mailing address: Mirian Strauss, Sección de Biología Celular, Instituto de Medicina Tropical, Universidad Central de Venezuela, Apartado 47019, Caracas 1041-A, Venezuela  
TEL: 58-212-6053650 FAX: 58-212-2434685  
E-mail: mstraussve@gmail.com

viability against adriamycin, confirming that Hsp27 does protect cardiac cells against adriamycin-induced toxicity<sup>10</sup>. Transgenic mice with cardiac-specific overexpression of Hsp27 attenuate adriamycin-induced cardiac dysfunction in mice<sup>11</sup>. The overexpression of Hsp20 inhibits adriamycin triggered cardiac injury possibly dependent on Akt kinase activation and the attenuation of oxidative stress<sup>12</sup>. However, important issues still remain unresolved including, the biological role of Hsp25 in structural cardiac organization *in vivo* during short and long term adriamycin intoxication and its relationship with myosin accumulation as a potential molecular event associated with cardiac protection induced by thermal stress. In this work, our aim was to evaluate the effect of hyperthermia *in vivo* by using an animal experimental model of adriamycin-induced very late cardiotoxicity set up with differences in mortality, body weight, ventricular wall thickness, cellular damage, Hsp25 and myosin accumulation among control and treated animals at 0, 4, 8 and 12 weeks after treatment.

## Materials and Methods

### Animals

Female Sprague-Dawley rats (n=80) at approximately 21–24 days of age and weighing 40–60 g were obtained from the Instituto Venezolano de Investigaciones Científicas (Caracas, Venezuela). The rats were allowed free access to standard diet and water *ad libitum* at room temperature, which was 23°C. The animals were kept according to the norms specified in the “Guide for the Care and Use of Laboratory Animals” of the U.S. National Institutes of Health (NIH publication No. 85–23, revised 1996) and related ethical regulations of the Universidad Central de Venezuela, Instituto de Medicina Tropical.

### Materials

The adriamycin was purchased from Badan (Caracas, Venezuela). All biochemical compounds and monoclonal antibodies were obtained from Sigma-Aldrich (St. Louis, MO, USA). The compounds for structural and ultrastructural studies were purchased from Electron Microscopy Sciences (Hatfield, PA, USA).

### Adriamycin treatment

The animals were randomized into the following four groups (n=20 each): the control (Control), adriamycin (Adr), temperature (Temp) and temperature-adriamycin (Temp-Adr) groups. The drug was injected *i.v.* in the caudal vein to a cumulative dose of 27 mg/kg body weight, divided into three sub-doses of 9 mg/kg body weight/0.1 ml/day applied at 3-day intervals. Each of the Control group rats was injected *i.v.* with 0.1 ml of sterile water, following the pattern protocol described in Fig. 1.

### Thermal stress

Much of the existing data regarding Hsp responses to stress fails to exclude the potential acute effects of anesthetic

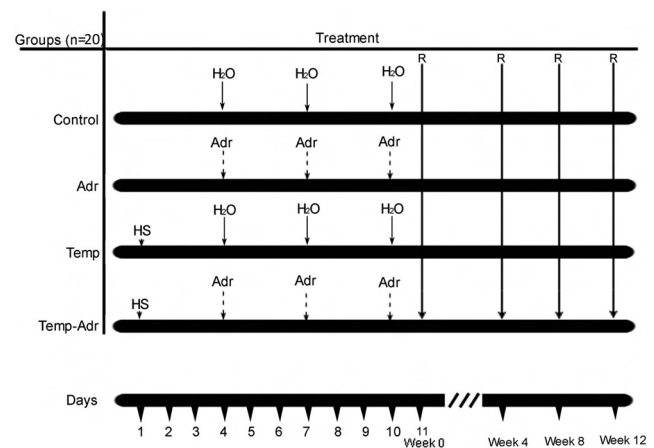


**Fig. 1.** Heat stress and drug administration protocol. The animals were randomized into the following four groups (n=20 each group): the control (Control), Adriamycin (Adr), Temperature (Temp) and Temperature-Adriamycin (Temp-Adr) groups. The rats of the control group were injected with sterile water (0.1 ml *i.v.*; H<sub>2</sub>O; arrow). Adriamycin was injected *i.v.* in three sub-doses of 9 mg/kg body weight/0.1 ml/day (Adr; dashed arrow) applied at 3-day intervals to a cumulative dose of 27 mg/kg body weight. The Temp-Adr group rats were exposed to a temperature of 45°C for 35 min (HS; arrowhead) prior to adriamycin treatment and allowed to recover at 23°C for 1 h. At 24 hours after the third adriamycin sub-dose 0, 4, 8 and 12 weeks after treatment, the hearts of the rats were removed (R; downwards arrow) for biometric, ultrastructural and biochemical studies.

agents used in experimental protocols<sup>13</sup> and the effects of immunomodulators on anti-Hsp antibodies<sup>14</sup>. Temp-Adr group rats were exposed to a temperature of 45°C for 35 min prior to adriamycin treatment, without anesthesia, in a padded wooden cage with thermal and humidity controls, after which they were allowed to recover at 23°C for 1h; a similar method has already been reported<sup>15</sup>. Finally, 24 hours after the third adriamycin sub-dose at weeks 0 and 4, 8, and 12 after treatment, the rats' hearts were removed for biometric, ultrastructural and biochemical studies (Fig. 1).

### Biometric study

Paraffin-embedded hearts were sectioned at 4- $\mu$ m intervals and stained with H&E. The sectioned free left ventricular walls were examined by light microscopy and drawn with an adapted *camera lucida*. The thicknesses of the free left ventricular walls were determined by means of SigmaScan image analysis software.

### Ultrastructural study

Left ventricular free wall samples were first fixed with Karnovsky's fixative (320 mosmol pH 7.4 for 2 h at 4°C), then post-fixed in osmic acid (0.12 M 2% osmium tetroxide, 320 mosmol, pH 7.4, for 2 h at 4°C), dissolved in a phosphate buffer (1 h at room temperature) and then dehydrated in acetone (50%, 70%, 80%, 95% and 100%; 30 min each).

Finally, they were embedded in polymerizing epoxy resin. After embedding, thin sections were cut, stained with saturated uranyl acetate (5 min) and lead citrate (3 min) and examined with a transmission electron microscope (Hitachi 300, 75 kV).

### Cellular damage

The percentage of cellular damage was interpreted following a semi-quantitative scoring cytogram system. Values ranging from 0–4 were assigned to four cellular damage zones observed in each grid (3 grids) for all experimental groups. In addition, 6 ultrastructural variables were taken into consideration (nucleus, contractile apparatus, mitochondria, endoplasmic reticulum, membranes, extracellular findings). After observation ( $\times 6300$ ), the 100% level of damage was related to a maximal theoretical value of 72 (4 damage zones  $\times$  3 grids  $\times$  6 ultrastructural variables)<sup>16</sup>.

### Western blot analysis

Free left wall ventricular tissue was homogenized (4°C; 1 ml extraction buffer, Tris-HCl 20 mM, EDTA 2 mM, PMSF 1 mM, pH 7.4) using a Potter-Elvehjem tissue grinder. The samples were centrifuged (14000 RPM/10 min), and the pellet was discarded. The Hsp25 and myosin content in the supernatant of the homogenized heart tissue was determined by Western blot analysis. Protein samples were diluted with a 4  $\times$  Laemmli buffer solution. Equal amounts of protein samples (20  $\mu$ g per lane) were applied to 10% polyacrylamide gels and separated by SDS-PAGE in duplicated gels using a Bio-Rad Mini-Gel system. One gel was stained with Coomassie Brilliant Blue G-250 to confirm the equivalence of loading concentrations and the adequacy of the sample preparation, while the second gel was transferred to a nitrocellulose membrane and stained with Ponceau Red before recognizing Hsp25 and myosin. Then, the membranes were washed in PBS (pH 7.4), 0.1% Tween 20 and 5% fat free milk to block non-specific binding sites and incubated with mouse monoclonal IgG against Hsp25 (Sigma, St. Louis, MO, USA; clone IAP-28) or myosin smooth muscle (Sigma, St. Louis, MO, USA; clone hSM-V) in a 1:500 dilution. After washing, a secondary antibody was used. The protein bands were detected using an enhanced chemiluminescent substrate and exposed to films. The relative levels of the protein bands were determined with the use of optical densitometry (GS-800 densitometer and the Quantity One Program; Bio-Rad).

### Statistical analysis

A 2-way analysis of variance (ANOVA) was undertaken to evaluate the similarities among the media of all the variables included in this study<sup>17</sup>. The Duncan's post hoc test (or multiple comparison test) can be used to determine the significant differences between group means in an ANOVA setting and is based on range statistics<sup>18</sup>. Statistically significant differences from the control and Adr groups are indicated with a dagger and double dagger respectively in Figs 2, 3, 4, 7 and 8.

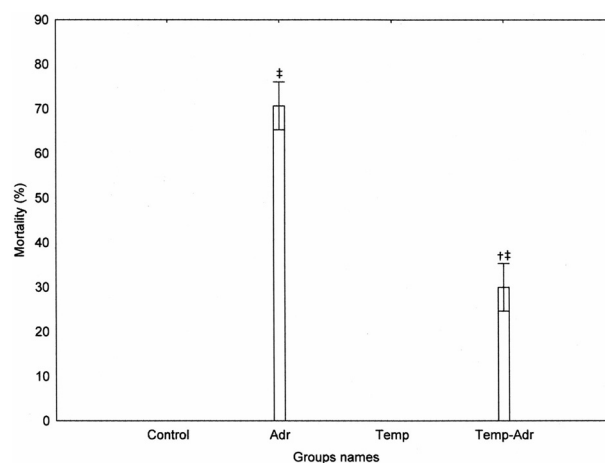


**Fig. 2.** Cumulative mortality during the experimental period for all groups. An increase in mortality was observed in the Adr group (75%) in contrast to the results of the Control, Temp and Temp-Adr rats, which showed 0, 0 and 30% mortality, respectively. The column corresponds to the mean cumulative mortality, and the whisker corresponds to the standard error. ANOVA and the Duncan post hoc test showed significance differences among groups ( $p < 0.05$ ).

The values showed in the Cartesian and bar graphs are expressed as standard errors of the mean. In addition, the statistical analysis of the data generated was also evaluated with a Principal Component Analysis (PCA) because of the multivariate condition of the experimental design. PCA describes the data behavior of the 4 groups, Control, Adr, Temp and Temp-Adr, at the times studied (0, 4, 8 and 12 weeks) as a function of the analyzed variables (mortality, body weight, left ventricular wall thickness, cell damage, Hsp25 OD/mm<sup>2</sup> and myosin OD/mm<sup>2</sup>) in a single rectangular Cartesian plane (biplot). The PCA was computed with the Multivariate Statistical Package (MVSP). The data generated was interpreted biologically<sup>19</sup>. The expected probability was fitted to  $p < 0.05$ .

## Results

### Mortality

In the Adr group, the cumulative mortality reached 75%, in contrast to the Control, Temp and Temp-Adr groups, where 0, 0 and 30% mortality was detected, respectively (Fig. 2).

### Body weight

The drug applied to the Adr group caused a significant reduction in body weight from week 4 compared with the Control group, which showed continuous weight gain throughout the experiment. The animals exposed to hyperthermia before treatment had a lower weight gain at weeks 4 and 12 compared with the Control rats. The Temp-Adr group experienced a decrease in body weight after week 4 until week 12 (Fig. 3).

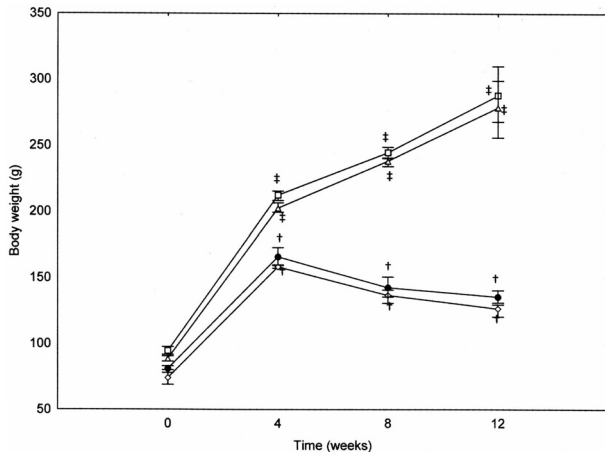


**Fig. 3.** Weight gain during the experimental period. Adriamycin caused a significant reduction in body weight from week 4 compared with the Control and Temp groups. The Temp-Adr group experienced a decrease in body weight from week 4 until week 12. The Control, Adr, Temp and Temp-Adr rats are indicated by empty squares, empty diamonds, empty triangles and full circles, respectively. Values are shown as the means  $\pm$  standard errors. ANOVA and Duncan post hoc test showed significance differences among groups ( $p < 0.05$ ). Statistically significant differences compared with the control and Adr groups are indicated with a dagger and double-dagger, respectively.

### Biometric study

The Adr and Temp-Adr groups experienced a reduction in the thickness of the left ventricular wall from week 8 to week 12 compared with the Control and Temp groups, respectively. The reduction for the Adr group seems to be bigger than that for the Temp-Adr group, both at 8 and 12 weeks. Nevertheless, no significant differences in left ventricular wall thickness were observed in the Control and Adr groups between 0 and 4 weeks after the beginning of the adriamycin treatment (Fig. 4).

### Ultrastructural study

In week 0 (Fig. 5 A–D), the left ventricular cardiac wall tissue samples from the Control (A), Adr (B), Temp (C) and Temp-Adr (D) groups all showed normal appearances. Four weeks after treatment (Fig. 5, E–H), a few changes were observed in the samples from the Adr (F) and Temp-Adr (H) groups including sarcomeric and mitochondrial modifications and the presence of vacuoles and lipid droplets, in contrast to the samples from Control (E) and Temp (G) groups. In addition, at 8 (Fig. 6 A–D) and 12 weeks (Fig. 6 E–H) after treatment, the Adr (B, F) and Temp-Adr (D, H) tissue samples showed a diffuse disarray of myofibrils and an abnormal pattern of the bands in the sarcomere, disorganization in the contractile element, degeneration of fibers and loss of the characteristic sarcomeric structure, giving the appearance of a lax tissue, as well as the presence of a signif-

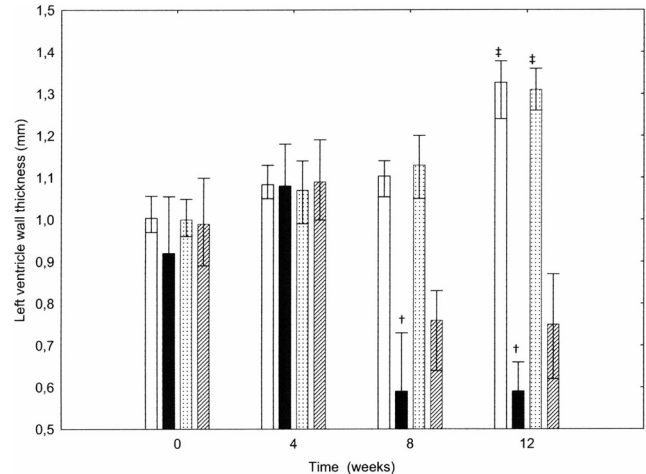


**Fig. 4.** Left ventricular wall thickness. The wall thickness reduction in the Adr group seems to be bigger than that in the Temp-Adr group at 8 and 12 weeks. The Control, Adr, Temp and Temp-Adr groups are indicated by white columns, black columns, dotted columns and slashed columns, respectively. Values are shown as the means  $\pm$  standard errors. ANOVA and Duncan post hoc test showed significance differences among groups ( $p < 0.05$ ). Statistically significant differences compared with the control and Adr groups are indicated with a dagger and double-dagger, respectively.

icant perinuclear edema and a perinuclear cistern exhibiting invaginations over its whole arrangement.

### Cellular damage

The resulting damage for each condition was expressed as a percentage of the maximal theoretical damage (Fig. 7). The Adr group showed the highest percentage of cellular damage in contrast to the samples from the Temp-Adr group, which had less cellular damage (8 and 12 weeks). However, the smallest amounts of damage were clearly observed in the Control and Temp groups.

### Western blot analysis

Compared with the Control group, the Adr group showed a notable increase in Hsp25 accumulation. Two bands in particular were recognized by the anti-Hsp25 antibody, corresponding to weeks 0 and 8 after adriamycin treatment. In contrast, the Temp-Adr group revealed the densest band recognized by the same antibody corresponding to week 0. Hsp25 was also recognized in the Temp group, especially at 0 and 8 weeks (Fig. 8A). Consistent with the highest accumulation of Hsp25, myosin also had its densest band in the Temp-Adr treated group at 0 week. This result was similar to that of the Temp group (0 week). However, the highest value of myosin was seen in the control group at week 4 as a result of the normal growth of the rats in this group. Myosin accumulation decreased more in both Adr treated groups from week 8. (Fig. 8B).

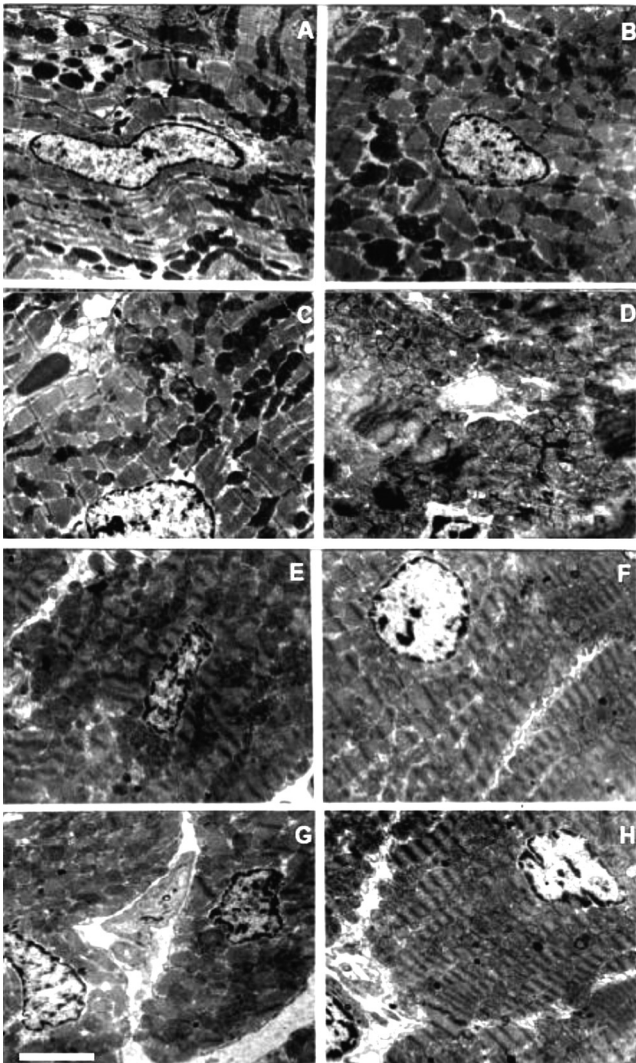


**Fig. 5.** Electron photomicrographs of free left wall ventricular cardiac tissue at 0 and 4 weeks after treatment. Cardiac tissue showed normal appearances in all four groups at 0 week (A–D). A small number of sarcomeric and mitochondria alterations and the presence of vacuoles and lipid droplets were observed in the ADR and Temp-ADR samples compared with the Control and Temp samples at 4 weeks (E–H) after treatment. Images A and E, B and F, C and G and D and H are of Control, ADR, Temp and Temp-ADR tissues, respectively (magnification,  $\times 6280$ ; scale bar= $2.3 \mu\text{m}$ ; taken with 75 kV).

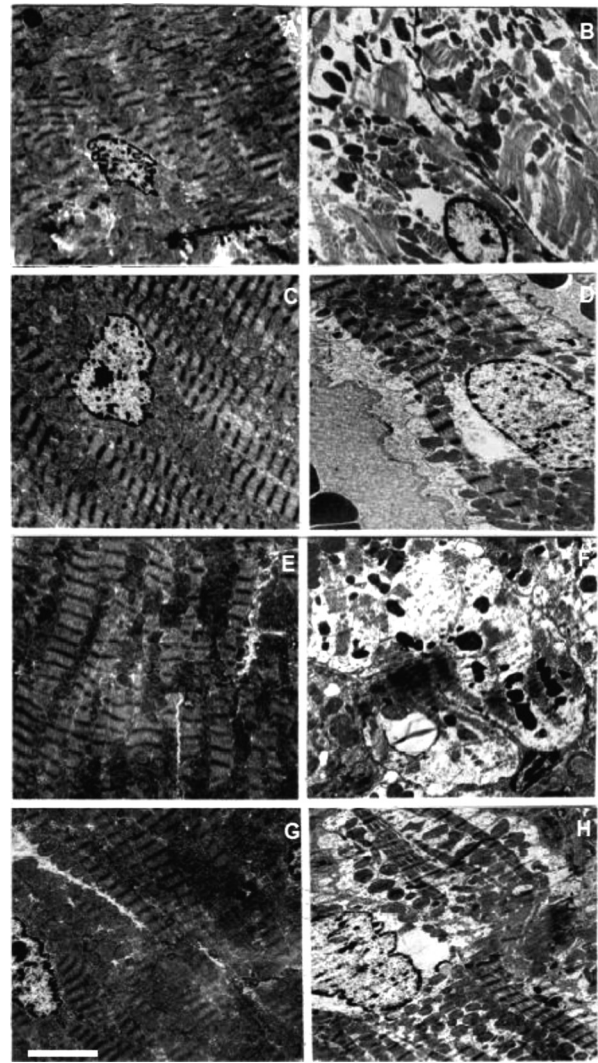


**Fig. 6.** Electron photomicrographs of left ventricular wall cardiac tissue at 8 and 12 weeks after treatment. Myofibrillar disarrangement, abundant intermyofibrillar spaces and disassembly, rupture and loss of myofibrils were observed in the ADR and Temp-ADR samples in contrast to the Control and Temp samples, which had normal patterns of cardiac tissue. The ADR group alterations seemed to be larger than those of the Temp-ADR group both at 8 and 12 weeks after treatment. Images A and E, B and F, C and G and D and H are of Control, ADR, Temp and Temp-ADR tissues, respectively (magnification,  $\times 6280$ ; scale bar= $2.3 \mu\text{m}$ ; taken with 75 kV).

### Statistical analysis

The ANOVA and Duncan post hoc test showed the differences among variables with  $p < 0.05$  in each of the analyzed variables. The PCA biplot represented the influence of each variable in a vectorial manner referred to as autovectors (Fig. 9). The autovectors indicated the direction and meaning of change in each variable. Autovectors pointing in the same direction correlated directly in the PCA model together with a similar change in the variables. Mortality and cell damage were clear examples. On the other hand, autovec-

tors pointing in opposite directions were inversely correlated. Mortality and cell damage were found to be antipodal variables for myosin expression. Body weight and left ventricle wall thickness were diametric variables, since the body weight loss was associated conversely with a reduction in the thickness of the left ventricle wall. The PCA model also quantitatively demonstrated that at the beginning of the experiments (0 weeks) there was a high Hsp25 accumulation and not much increase in body weight. From 4 to 12 weeks, the Hsp25 accumulation diminished and body weight

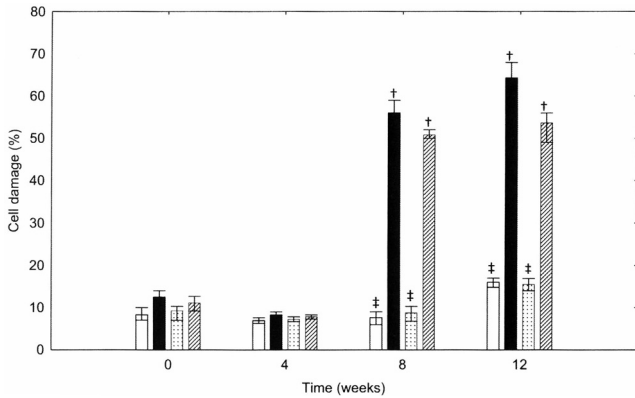


**Fig. 7.** Cellular damage of left ventricular wall cardiac tissue. The Adr group showed the highest percentage of cellular damage in contrast to the Temp-Adr samples, which had the least cellular damage (8 and 12 weeks). The percentage of cellular damage was interpreted following a semi-quantitative scoring cytogram system. Values ranging from 0–4 were assigned to cellular damage zones for all four groups. The 100% level of damage was related to the maximal theoretical value of 72. The Control, Adr, Temp and Temp-Adr groups are indicated by white columns, black columns, dotted columns and slashed columns, respectively. Values are shown as the means  $\pm$  standard errors. ANOVA and Duncan post hoc test showed significance differences among groups ( $p < 0.05$ ). Statistically significant differences compared with the control and Adr groups are indicated with a dagger and double-dagger, respectively.

increased.

**Discussion**

In this study, we demonstrated that heat stress preconditioning of adriamycin-treated rats led to a remarkable increase in Hsp25 accumulation. This first cellular response was directly linked to an increase of myosin in addition to fewer cardiac subcellular toxic injuries. Stress response involves the rapid and transient increase in a specific set of Hsps<sup>20</sup>, and in this sense, protein transcription and translation are halted, presumably to alleviate the burden of misfolded proteins in the cell<sup>21</sup>. Although Hsp25 was induced by hyperthermia, we did not compare the Hsp25 accumulation to others Hsps. However, our observations could not exclude the role of others Hsps because, for example, overexpression of Hsp27 in the human heart upregulated both Hsp32 and Hsp70 expression in response to adriamycin treatment<sup>11</sup>. In this regard, mice deficient in alpha-B-crystallin and HspB2 (two small Hsps related to Hsp25) show decreased total glutathione levels in the heart and increased susceptibility to ischemia-reperfusion-induced damage, whereas mice overexpressing alpha-B-crystallin show increased resistance against ischemia-reperfusion<sup>22</sup>. Increased expression of Hsp20 protects the heart from ischemia-reperfusion-induced injury, leading to restoration of cardiac function and reduced infarction<sup>23</sup>.

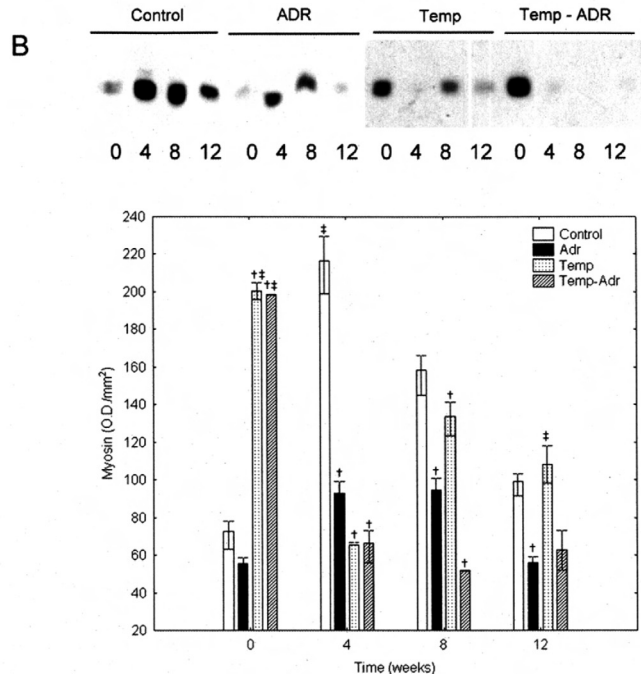
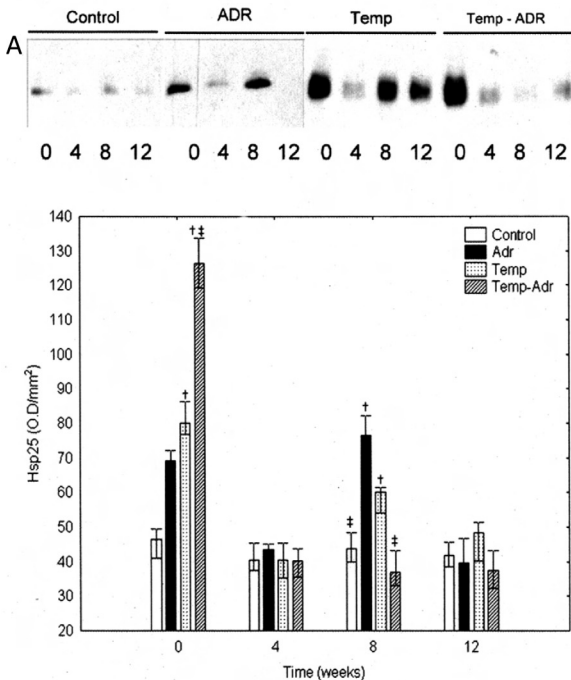


**Fig. 8.** Western blot analysis of Hsp25 and myosin accumulation. In the Adr group, two bands were recognized by the anti-Hsp25 antibody at 0 and 8 weeks after treatment. The Temp-Adr group had the densest band recognized by the same antibody (week 0) (A). Consistent with the highest accumulation of Hsp25, myosin also had its densest band in the Temp-Adr-treated group at 0 week. This result was similar to that in the Control group at 4 weeks and to that of the Temp group at week 0. Myosin accumulation decreased more in both Adr-treated groups from week 8 (B). The Western blot analysis is shown above the densitometric analysis. The Control, Adr, Temp and Temp-Adr groups are indicated by white columns, black columns, dotted columns and slashed columns, respectively. Values are shown as means  $\pm$  standard error. ANOVA and Duncan post hoc test showed significance differences among groups ( $p < 0.05$ ). Statistically significant differences compared with the Control and Adr groups are indicated with a dagger and double-dagger, respectively.

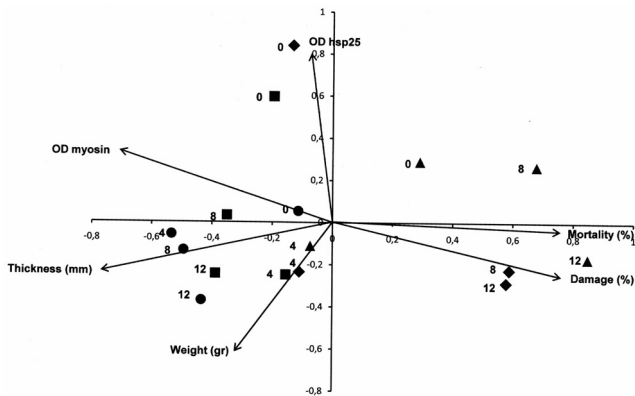


**Fig. 9.** Cartesian representation of the Principal Components Analysis. Mortality and cell damage were directly correlated, while Hsp25, left ventricular wall thickness and myosin autovectors pointed in the opposite direction. Mortality and cell damage were antipodal variables for myosin. Each symbol is associated with a number (representing time in weeks) and a letter (symbolizing the groups). The Control, Adr, Temp and Temp-Adr groups are indicated by filled triangles, filled squares, filled circles and filled diamonds, respectively. The arrowed lines correspond to autovectors; each autovector matches with a variable (mortality, body weight, left ventricular wall thickness, cell damage, myosin and Hsp25 accumulation).

On the other hand, the recognition of Hsp25 in Adr samples (0 and 8 weeks) may be associated with two different stress-stimuli responses: the heart adriamycin toxic injury immediately after treatment, and a reduction of left ventricular wall thickness 8 weeks after treatment. Moreover, the parallelism between the accumulation of Hsp25 and myosin in the Temp-Adr treated heart (0 week) suggests temperature-associated cardioprotection. However, the diminution of myosin accumulation at week 8 could be related to a significant reduction in the left ventricular wall thickness and the higher percentage of subcellular damage. This is in contrast to the observations for the control rats, which grew normally and showed continuous accumulation of myosin throughout the experiment.

The development of heat stress response has been extensively studied in order to characterize the different steps of this form of preconditioning. It appears that chemical signal indications (such as nitric oxide and reactive oxygen species, ROS) released by sublethal hyperthermic stress trigger a complex cascade of signalling events that include activation of protein kinase C (PKC) and mitogen-activated protein kinases (MAPK) and culminate in increased synthesis of inducible nitric oxide synthase, cyclooxygenase-2, antioxidant enzymes and protective proteins, such as heat stress proteins<sup>24</sup>. Hyperthermia protects cells from adriamycin-induced death through induction and phosphorylation of small Hsps and its antiapoptotic and actin-remodeling activities<sup>25</sup>. The small Hsps, including human Hsp27 and the mouse homolog Hsp25, have been shown to protect different

types of cells against oxidative stress. Hsp25 may play an important role in maintenance of muscle homeostasis, regulation of the glutathione system and resistance to ROS in muscle cells. Moreover, Hsp25 overexpression above a certain threshold aids significant improvement of cardiac morphology and histological appearance, as demonstrated by decreased fibrosis and calcification and preservation of tissue integrity<sup>26</sup>.

However, the issue of whether Hsps or antioxidant enzymes are the primary end-effector of this cardioprotection continues to be a matter of debate<sup>8</sup>. There is increasing evidence that alpha-Hsps are concerned with functions other than chaperoning. Several studies demonstrate an interaction between alpha-Hsps and nucleic acids. It is known that an overexpression of Hsp27 in cells can promote the accelerated recovery of heat shock-produced intranuclear protein aggregates<sup>27</sup>. An involvement of Hsp25 granules in binding and targeting denatured substrates for accelerated degradation has also been shown. Data revealing that the Hsp25-luciferase granules are stained positively with antibodies to components of the proteasome are supportive of such an idea<sup>28</sup>. Correlation between the total cellular level of Hsp25 phosphorylation and the formation of nuclear granules has been shown. Dephosphorylated alpha-Hsps seem to be very versatile protective agents, that play a dual role in protein and membrane protection and might also be involved in the preservation of nucleic acid<sup>29</sup>. On the other hand, although Hsp25 expression levels are quite high in mature tissue, the developmental regulation of expression appears to be of significant importance; therefore, developmentally associated changes cannot be completely discriminated<sup>30</sup>.

Adriamycin affects the expression and content of myocardial structural and regulatory proteins, including that of alpha-myosin heavy chain, ventricular myosin light chain-2 isoform, brain natriuretic peptide and in particular, myosin light chain kinase (MLCK), which may disturb the control of coronary vessels<sup>31,32</sup>. In support of these results, in adriamycin-treated rats previously protected with L-carnitine, which promotes Hsp70 and Hsp25<sup>33,33</sup> we observed remarkable recognition with anti-myosin light chain kinase (unpublished results). Moreover, the most common abnormality in patients treated with adriamycin was the increased afterload<sup>34</sup> exclusively attributable to reduced left ventricular wall thickness. In this regard, acute pressure overload alters cardiac gene expression by mechanisms that selectively regulate the translational activity of specific mRNAs. Expression of many genes is also dependent on how efficiently each mRNA is translated<sup>35</sup>.

The direct effect of chronic adriamycin treatment on the level of the contractile machinery provides an additional mechanism through which anthracyclines exert their debilitating cardiotoxic effects<sup>36</sup>. The decreased contractility of individual myocytes may relate to their low myosin content and could contribute to the reduced cardiac output produced by adriamycin treatment<sup>37</sup>. The demonstration that cardiac sarcomeric myosin organization is more noticeably perturbed than myosin IIB or f-actin organization raises the



intriguing possibility that cardiac sarcomeric myosin may be a specific target that contributes to the unique sensitivity of cardiac tissue to the toxic effects of adriamycin<sup>38</sup>. Both myosin and Hsp25 genes are developmentally regulated. This regulation has been reported for the genes encoding the MLC genes, MLCIA and MLCIV. In addition, the two MHC proteins, called MHC $\alpha$  and MHC $\beta$ , are developmentally and hormonally regulated as well as in response to cardiac hypertrophy due to hemodynamic overload<sup>39</sup>.

In this work, as a contribution to understanding the biological role of Hsp25 induced by thermal stress and its relationship with myosin accumulation, the biologically connected events herein discussed were mathematically integrated by the biometrical and multivariate approaches. Even though the possible protection provided by the hyperthermic strategy was not evident in the univariate analysis of each variable, the PCA model proved the positive correlation between Hsp25 accumulation, the thickness of the left ventricular wall and myosin accumulation. In addition, mortality and cell damage were found to be inversely correlated with the accumulation of myosin. Despite the PCA model robustness, a few inconsistencies became evident, since the natural process compared with the mathematical reduction includes many more unknown variables. However, the PCA model represents a powerful technique in the approach to research of biological systems. Based on the induction of Hsp25 and the myosin accumulation, which may enhance the cell-protecting mechanism, hyperthermia needs further investigation as a possible cardioprotective strategy.

**Acknowledgments:** This work was supported by LOCTI-UCV (Laboratorios ELMOR S.A.) and the Consejo de Desarrollo Científico y Humanístico (CDCH) from the Universidad Central de Venezuela. We thank Prof Phillip Shultz for his valuable help with the English.

## References

- Buzdar A, Marcus C, Smith T, and Blumenschein G. Early and delayed clinical cardiotoxicity of doxorubicin. *Cancer*. **55**: 2761–2765. 1985.
- Kalivendi S, Kotamraju S, Zhao H, Joseph J, and Kalyanaraman B. Doxorubicin-induced apoptosis is associated with increased transcription of endothelial nitric-oxide synthase. Effect of antiapoptotic antioxidants and calcium. *J Biol Chem*. **276**: 47266–47276. 2001.
- Strauss M, Anselmi G, Hermoso T, and Tejero F. Carnitine promotes heat shock protein synthesis in Adriamycin-induced cardiomyopathy in a neonatal rat experimental model. *J Mol Cell Cardiol*. **30**: 2319–2325. 1998.
- Joyeux M, Godin-Ribuot D, Faure P, Demenge P, and Ribuot C. Heat stress protects against electrophysiological damages induced by acute doxorubicin exposure in isolated rat hearts. *Cardiovasc Drugs Ther*. **15**: 219–224. 2001.
- Ito H, Miller S, Billingham M, Akimoto H, Torti S, Wade R, Gahlmann R, Lyons G, Kedes L, and Torti FM. Doxorubicin selectively inhibits muscle gene expression in cardiac muscle cells in vivo and in vitro. *Proc Natl Acad Sci USA*. **87**: 4275–4279. 1990.
- Thompson KL, Rosenzweig BA, Zhang J, Knapton AD, Honchel R, Lipshultz SE, Retief J, Sistare FD, and Herman EH. Early alterations in heart gene expression profiles associated with doxorubicin cardiotoxicity in rats. *Cancer Chemother Pharmacol*. **66**: 303–314. 2010.
- Akimoto H, Bruno N, Slate D, Billingham M, Torti S, and Torti F. Effect of verapamil on doxorubicin cardiotoxicity: altered muscle gene expression in cultured neonatal rat cardiomyocytes. *Cancer Res*. **53**: 4658–4664. 1993.
- Xi L, Tekin D, Bhargava P, and Kukreja R. Whole body hyperthermia and preconditioning of the heart: basic concepts, complexity and potential mechanisms. *Int J Hyperthermia*. **17**: 439–455. 2001.
- Sardao VA, Oliveira PJ, Holy J, Oliveira CR, and Wallace KB. Morphological alterations induced by doxorubicin on H9c2 myoblasts: nuclear mitochondrial and cytoskeletal targets. *Cell Biol Toxicol*. **25**: 227–243. 2009.
- Turakhia S, Venkatakrishnan CD, Dunsmore K, Wong H, Kuppusamy P, Zweier JL, and Ilangoan G. Doxorubicin-induced cardiotoxicity: direct correlation of cardiac fibroblast and H9c2 cell survival and aconitase activity with heat shock protein 27. *Am J Physiol Heart Circ Physiol*. **293**: H3111–H3121. 2007.
- Liu L, Zhang X, Qian Bo, Min X, Gao X, Li Ch, Cheng Y, and Huang J. Over-expression of heat shock protein 27 attenuates doxorubicin-induced cardiac dysfunction in mice. *Eur J Heart Fail*. **9**: 762–769. 2007.
- Fan GC, Zhou X, Wang X, Song G, Qian J, Nicolaou P, Chen G, Ren X, and Kranias EG. Heat shock protein 20 interacting with phosphorylated Akt reduces doxorubicin-triggered oxidative stress and cardiotoxicity. *Circ Res*. **103**: 1270–1279. 2008.
- Kilgore J, Ross C, and Saunders D. Potential effects of anaesthetic agents on heat shock proteins in the laboratory rat. *Texas J Sci*. **55**: 149–158. 2003.
- Colucci D, Ferrero P, Ferreira P, Elena G, and Puig N. Efectos de la anestesia con sevoflurano sobre la respuesta inmunitaria y parámetros bioquímicos en ratones. Comparación entre exposición única y anestesia reiterada. *Rev Esp Anestesiol Reanim*. **50**: 170–175. 2003.
- Uehara K, Goto K, Kobayashi A, Kojima T, Akema T, Sugiura T, Yamada S, Ohira Y, Yoshioka T, and Aoki H. Heat stress enhances proliferative potential in rat soleus muscle. *Jap J Physiol*. **54**: 236–271. 2004.
- Palacios E, Carrasco HA, Scorza C, Rangel A, Inglessis G, and Fuenmayor A. Utilidad de la Biopsia Septal endomiocárdica en la enfermedad de Chagas. Resúmenes IX Congreso Sudamericano de Cardiología Caracas. **111**. 1979.
- Sokal R and Rohlf F. *Biometry: The Principles and Practices of Statistics in Biological Research*. 3rd ed. WHFreeman, Philadelphia. 1995.
- Winer BJ, Brown DR, and Michels KM. *Statistical Principles in Experimental Design*. Mc Graw-Hill, New York. 1991.
- Jolliffe I. *Principal Component Analysis*. Springer-Verlag, New York. 1986.
- Frier BC and Locke M. Heat stress inhibits skeletal muscle hypertrophy. *Cell Stress Chaperones*. **12**: 132–141. 2007.
- Fulda S, Gorman A, Hori O, and Samali A. Cellular stress response: cell survival and cell death. *Inter J Cell Biol*. Doi: 10.1155/2010/214074, 2010.
- Morrison LE, Whittaker RJ, Klepper RE, Wawrousek EF,



- and Glembotski CC. Roles for alphaB-crystallin and HSPB2 in protecting the myocardium from ischemia-reperfusion-induced damage in a KO mouse model. *Am J Physiol Heart Circ Physiol.* **286**: H847–H855. 2004.
23. Fan GC, Ren X, Qian J, Yuan Q, Nicolaou P, Wang Y, Jones K, Chu G, and Kranias E. Novel cardioprotective role of a small heat-shock protein, Hsp20, against ischemia/reperfusion injury. *Circulation.* **111**: 1792–1799. 2005.
  24. Joyeux-Faure M, Arnaud C, Godin-Ribuot D, and Ribuot C. Heat stress preconditioning and delayed myocardial protection: what is new. *Cardiovascular Res.* **69**: 469–477. 2003.
  25. Venkatakrishnan CD, Tewari AK, Moldovan L, Cardounel AJ, Zweier JL, Kuppusamy P, and Ilangovan G. Heat shock protects cardiac cells from doxorubicin-induced toxicity by activating p38 MAPK and phosphorylation of small heat shock protein 27. *Am J Physiol Heart Circ Physiol.* **291**: H2680–H2689. 2006.
  26. Escobedo J, Pucci M, and Koh T. Hsp25 protects skeletal muscle cells against oxidative stress. *Free Rad Biol Med.* **37**: 1455–1462. 2004.
  27. Kampinga HH, Brunsting JF, Stege GJ, Konings AW, and Landry J. Cells overexpressing Hsp27 show accelerated recovery from heat-induced nuclear protein aggregation. *Biochem Biophys Res Commun* **204**: 1170–1177. 1994.
  28. Bryantsev AL, Loktionova SA, Ilyinskaya OP, Tararak EM, Kampinga HH, and Kabakov AE. Distribution, phosphorylation, and activities of Hsp25 in heat-stressed H9c2 myoblasts: a functional link to cytoprotection. *Cell Stress Chaperones.* **7**: 146–155. 2002.
  29. Narberhaus F. Alfa-crystallin-type heat shock proteins: socializing minichaperones in the context of a multichaperone network. *Microbio Mol Biol Rev.* **66**: 64–93. 2002.
  30. Nadal-Ginard B and Mahdavi V. Molecular basis of cardiac performance. Plasticity of the myocardium generated through protein isoform switches. *J Clin Invest.* **84**: 1693–1700. 1989.
  31. Ito T, Muraoka S, Takahashi K, Fujio Y, Schaffer SW, and Azuma J. Beneficial effect of taurine treatment against doxorubicin-induced cardiotoxicity in mice. *Adv Exp Med Biol.* **643**: 65–74. 2009.
  32. Dudnakova TV, Lakomkin VL, Tsyplenkova VG, Shekhonin BV, Shirinskii VP, and Kapelko VI. Effect of Adriamycin on expression and content of myocardial structural and regulatory proteins. *Kardiologiya.* **42**: 60–66. 2002.
  33. Porras N, Strauss M, Rodriguez M, and Anselmi G. Hsp70 accumulation and ultrastructural features of lung and liver induced by ethanol treatment with and without L-carnitine protection in rats. *Exp Toxicol Pathol.* **57**: 227–237. 2006.
  34. Lipshultz S, Colan SD, Gelber RD, Perez-Atayde AR, Sallan SE, and Sanders SP. Late cardiac effects of Doxorubicin therapy for acute lymphoblastic leukaemia in childhood. *N Engl J Med.* **324**: 808–815. 1991.
  35. Spruill LS, Baicu CF, Zile MR, and McDermott PJ. Selective translation of mRNAs in the left ventricular myocardium of the mouse in response to acute pressure overload. *J Mol Cell Cardiol.* **44**: 69–75. 2008.
  36. Bottone A, Voest E, and de Beer E. Impairment of the actin-myosin interaction in permeabilized cardiac trabeculae after chronic doxorubicin treatment. *Clin Cancer Res.* **4**: 1031–1037. 1998.
  37. Jones SM, Kirby MS, Harding SE, Vescova G, Wanless RB, Dalla Libera LD, and Poole-Wilson PA. Adriamycin cardiomyopathy in the rabbit: alterations in contractile proteins and myocyte function. *Cardiovasc Res.* **24**: 834–842. 1990.
  38. Dudnakova TV, Lakomkin VL, Tsyplenkova VG, Skehoriu BV, Shininsky VP, and Kapelko VI. Alterations in myocardial cytoskeletal and regulatory protein expression following a single Doxorubicin injection. *J Cardiovasc Pharmacol.* **41**: 788–794. 2003.
  39. Lyons GE, Schiaffino S, Sassoon D, Barton P, and Buckingham M. Developmental regulation of myosin gene expression in mouse cardiac muscle. *J Cell Biol.* **111**: 2427–2436. 1990.